Direct Interactions and the $^6Li + {}^6Li \rightarrow \alpha + \alpha + \alpha$ Reaction*

L. L. Gadeken† and E. Norbeck
Department of Physics and Astronomy, The University of Iowa, Iowa City, Iowa 52240
(Received 14 February 1972)

The interaction of ^{6}Li with ^{6}Li was found to yield three ^{4}He nuclei via a direct process, as well as through intermediate ^{8}Be states. Large peaks attributed to direct interactions were observed in the experimental data at bombarding energies of 2.0, 6.0, and 13.0 MeV. These peaks were fitted using a simple model which assumed an $\alpha + d$ cluster structure for the ^{6}Li nuclei and an interaction potential which acted only between the deuterons.

1. INTRODUCTION

When two nuclei interact and rearrange so as to produce three nuclei, the reaction often goes in two steps, where the second is the breakup of an unstable intermediate nucleus. We present data[1] for the $2\ ^6\text{Li} \rightarrow 3\alpha$ reaction which show that the cross section for a one-step process is appreciably greater than that for the formation and subsequent decay of a ^{8}Be nucleus. In the theoretical model which is used to fit the data, the α particles are not allowed to interact and thus no intermediate ^{8}Be nucleus can be formed. The model predicts a maximum yield when one of the three α particles experiences no momentum transfer during the course of the reaction. If this α particle comes from the beam, it is found at small angles moving with a velocity equal to that of the beam. If it comes from the target, it leaves the reaction with zero energy. This feature is also characteristic of quasielastic scattering.[2] One feature of the reaction described here that is not shared by the quasielastic types is the production of two high-energy particles by what could be called a two-nucleon-transfer process.

The first experimental indication that a one-step process was occurring in the $2\ ^6\text{Li} \rightarrow 3\alpha$ reaction was published by Kamegai.[3] He found a large enhancement in the cross section where two of the α particles shared almost all of the available energy. Since he used only one beam energy (2.0 MeV) and had only limited resolution, his results were compatible with the assumption of a state at about 20 MeV in ^{8}Be. He emphasized, however, that this hypothesis would require the cross section for the production of such a state to be 23 times that of the ground state.

Berkowitz, in a more thorough study of the same reaction,[4] looked for the process described here by searching for evidence of α particles with zero momentum transfer. He saw large peaks in approximately the right regions, but could not determine with certainty whether this process was occurring or not. He did not have a theoretical expression for the cross section as a function of angle and energy to compare with his data, and the angular uncertainties and cumulative errors in the experiment prohibited the necessary quantitative study of the data as a function of momentum transfer.

Frois *et al.*[5] used the hypothesis of a quasimolecular state in the ^{6}Li-^{6}Li system to fit their single-parameter, α-particle energy spectra. Their model resembles in some ways the one presented here, but it is not clear how it could be extended to predict the α-α angular correlations.

2. THEORETICAL MODEL

The model had detail sufficient to include the essential features of the reaction, but did not include any extra features to help improve the fit to the data. A brief outline of the model is as follows: The final state consisted of three plane-wave α particles. The initial state contained two plane-wave ^{6}Li nuclei. Each ^{6}Li nucleus had a cluster structure composed of an α particle and a deuteron bound by a square-well potential. The interaction potential was a point interaction between the two deuterons; there was no interaction between the α particles.

For convenience all computations were performed in the lab system. Consider a three-body reaction, $B + T \rightarrow F + P + U$. The differential cross section for particle F, i.e., the energy spectrum when particle F is detected in a detector with solid angle, Ω_F, at an angle of θ_F and particle P is detected in a detector with solid angle, Ω_P, at an angle of θ_P, may be written in the form

$$\frac{d^3\sigma}{d\Omega_F d\Omega_P dE_F} = \frac{2\pi}{\hbar^2}\frac{\mu}{k}\rho(E_F)|M|^2, \tag{1}$$

where μ is the reduced mass, $m_B m_T/(m_B + m_T)$, and $\hbar k$ is the relative momentum of the beam and target particles. The phase-space factor, ρ, is

given in terms of the particle momenta,[6]

$$\rho(E_F)=\frac{1}{(2\pi\hbar)^6}\,\frac{m_F m_P m_U p_F p_P{}^3}{(m_P+m_U)p_P{}^2+m_P(\vec{p}_F-\vec{p}_B)\cdot\vec{p}_P}\ . \tag{2}$$

The matrix element, M, between the initial and final states in the plane-wave Born approximation is

$$M=\langle\psi_f|\,V\,|\psi_i\rangle\ .$$

In this model we assumed that the only interaction which occurred during the reaction was the formation of an α particle by the two deuterons from the ^{6}Li nuclei. The nuclear potential, V, was taken to be a zero-range potential between the deuterons,

$$V=V_d\delta(\vec{d}_B-\vec{d}_T)\ .$$

The initial state was approximated by products of internal wave functions and incoming plane waves,

$$\psi_i=\Phi_{^6\mathrm{Li}}(\vec{d}_B-\vec{\alpha}_B)e^{i\vec{k}_B\cdot\vec{L}_B}\Phi_{^6\mathrm{Li}}(\vec{d}_T-\vec{\alpha}_T)e^{i\vec{k}_T\cdot\vec{L}_T}\ ,$$

and the final state by products of outgoing plane waves and an internal wave function for the α particle which was formed from the deuterons,

$$\psi_f=e^{i\vec{K}_B\cdot\vec{\alpha}_B}e^{i\vec{K}_T\cdot\vec{\alpha}_T}e^{i\vec{K}_d\cdot\vec{\alpha}_d}\Phi_\alpha(\vec{d}_B-\vec{d}_T)\ .$$

The coordinate definitions are shown in Fig. 1. Vectors $\vec{d}_B$ and $\vec{d}_T$ locate the deuterons in the beam and target nuclei, respectively. Vectors $\vec{\alpha}_B$, $\vec{\alpha}_T$, and $\vec{\alpha}_d$ point to the α particles. In terms of these coordinates the centers of mass of the ^{6}Li nuclei are

$$\vec{L}_{B,T}=\vec{\alpha}_{B,T}+\frac{m_d}{m_\alpha+m_d}(\vec{d}_{B,T}-\vec{\alpha}_{B,T})\ .$$

The independent set of variables chosen to facilitate the integration was

$$\vec{d}_B=\vec{d}_B\ ,$$
$$\vec{r}_d=\vec{d}_B-\vec{d}_T\ ,$$
$$\vec{r}_B=\vec{d}_B-\vec{\alpha}_B\ ,$$
$$\vec{r}_T=\vec{d}_T-\vec{\alpha}_T\ .$$

When the appropriate substitutions were made, the expression for the matrix element became

$$\begin{aligned}M=&\int d\vec{d}_B\,e^{i(\vec{k}_B+\vec{k}_T-\vec{K}_B-\vec{K}_T-\vec{K}_d)\cdot\vec{d}_B}\\&\times V_d\int d\vec{r}_d\ \delta(\vec{r}_d)\Phi_\alpha(\vec{r}_d)\,e^{-i[\vec{k}_T-(\vec{K}_T+\frac{1}{2}\vec{K}_d)]\cdot\vec{r}_d}\\&\times\int d\vec{r}_B\ \Phi_{^6\mathrm{Li}}(\vec{r}_B)\,e^{-i(\vec{k}'_B-\vec{K}_B)\cdot\vec{r}_B}\\&\times\int d\vec{r}_T\,\Phi_{^6\mathrm{Li}}(\vec{r}_T)\,e^{-i(\vec{k}'_T-\vec{K}_T)\cdot\vec{r}_T}\ ,\end{aligned}\tag{3}$$

where $\vec{k}'_{B,T}=m_\alpha\vec{k}_{B,T}/(m_\alpha+m_d)$. The first integral of Eq. (3) contains the requirement for conservation of momentum in the reaction. The second integral was made into a constant by the choice of a δ function for the potential between the two deuterons. This was justified by noting that the α-particle wave function, $\Phi_\alpha(\vec{r}_d)$, is strongly peaked about the origin as a function of the internal deuteron coordinates. Thus, even for a potential other than a δ function, the value of the integral would be only a slowly varying function of the momentum transfer. To obtain specific expressions for the internal ^{6}Li wave functions so that the third and fourth integrals of Eq. (3) could be evaluated, the nucleons in each ^{6}Li nucleus were postulated to have a cluster structure composed of an α particle and a deuteron bound by a square-well potential. Antisymmetrization effects were incorporated by

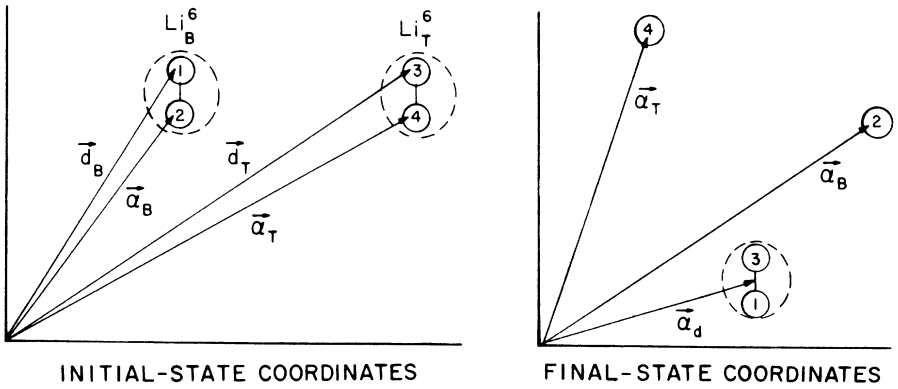

FIG. 1. Coordinates for the theoretical model.

using a 2S wave function, as explained by Wildermuth.[7] The third and fourth integrals of Eq. (3) are each given by:

$$g(\Delta)=\left(\frac{2\beta}{1+\beta R}\right)^{1/2}\frac{1}{\Delta}\left\{\frac{\sin[(\gamma-\Delta)R]}{2(\gamma-\Delta)}-\frac{\sin[(\gamma+\Delta)R]}{2(\gamma+\Delta)}+\frac{\sin\gamma R}{(\beta^2+\Delta^2)}(\beta\sin\Delta R+\Delta\cos\Delta R)\right\},$$

where

$$\gamma=\left[\frac{2m}{\hbar^2}(V_0-E_B)\right]^{1/2},\quad \beta=\left(\frac{2m}{\hbar^2}E_B\right)^{1/2},$$

and R is the radius of the square well, V_0 is its depth, and E_B is the binding energy and m the reduced mass of the $\alpha+d$ cluster.

The functional form of the matrix element may be shown by rewriting Eq. (3) as

$$M=V_d' g(|\vec{k}_B'-\vec{K}_B|)g(|\vec{k}_T'-\vec{K}_T|).$$

The symmetrization of the wave functions gave the complete matrix element which has the form

$$\begin{aligned}M=V_d'\{&g(|\vec{k}_B'-\vec{K}_B|)[g(|\vec{k}_T'-\vec{K}_T|)+g(|\vec{k}_T'-\vec{K}_d|)]\\&+g(|\vec{k}_B'-\vec{K}_T|)[g(|\vec{k}_T'-\vec{K}_B|)+g(|\vec{k}_T'-\vec{K}_d|)]\\&+g(|\vec{k}_B'-\vec{K}_d|)[g(|\vec{k}_T'-\vec{K}_B|)+g(|\vec{k}_T'-\vec{K}_T|)]\end{aligned}\qquad(4)$$

The laboratory energy spectrum of particle F predicted by this model was given by the expression which resulted when Eqs. (4) and (2) were substituted into Eq. (1).

The only free parameter in the theoretical model was the radius of the square well. The value $R=3.2$ fm ($V_0=-38.2$ MeV) was chosen for the calculations. The results were essentially the same in the range 2.4 fm $<R<$ 4.0 fm for the bombarding energies which were studied. This suggested that the shape of the nuclear potential for the ^{6}Li nuclei was not a critical factor and that the relatively sharp peaks of the calculated energy spectra were produced by the long tail of the bound-state wave function.

3. EXPERIMENT DESCRIBED

The data which initiated this study were taken for a different purpose at a beam energy of 6.0 MeV by F. D. Ingram. The experimental arrangement was similar to that previously described.[8] Two small detectors were fixed at $\theta_{F_1}=+15°$ and $\theta_{F_2}=+30°$ on one side of the scattering chamber and a movable 30° wide position-sensitive detector was located on the other side of the chamber. Data were obtained at all angles in the ranges $-10° < \theta_P < -170°$ (θ_{F_1}) and $-25° < \theta_P < -150°$ (θ_{F_2}) for coincident events between the position detector and one or the other of the fixed detectors. A detailed analysis showed that there was a large anomalous peak in each of the fixed-detector energy spectra for a narrow angular range (~40°) near $\theta_P = -160°$ (θ_{F_1}) and $\theta_P = -140°$ (θ_{F_2}).

It was found that these peaks corresponded to no known levels in the ^{8}Be nucleus if the assumption of sequential decay was invoked. However, the energies and angles of the peaks were correctly given if a direct interaction was assumed for which zero-momentum transfer to the beam α particle occurred.

Additional experimental data were obtained so that the theoretical model could be tested in detail. Two detectors were used: a small fixed detector with circular apertures which subtended a 5° angle relative to the center of the target and a larger position-sensitive detector with a rectangular aperture which spanned an angle of 31° in the reaction plane. Each coincident event in the detectors corresponding to a three-body nuclear reaction gave three pieces of information: the energy, E_F, of the particle incident on the fixed detector, the energy, E_P, and the angle, θ_P, of the particle incident on the position detector.

The use of a position detector is clearly advantageous in coincidence experiments of this type. The running time is greatly reduced, since data are collected simultaneously at a number of different angles. Plotting θ_P versus E_F is valuable, since variations of the E_F spectrum are shown as a continuous function of angle. Details become evident which might otherwise be overlooked.

The theoretical model predicted that for a fixed detector angle of $\theta_F=+30°$, the anomalous peaks in the E_F spectra would rise and fall as a function of angle only in the range from $-120° < \theta_P < -150°$ for $E_B=2.0$ MeV to $-70° < \theta_P < -145°$ for $E_B=13.0$ MeV. Runs were made at the following beam energies and position detector angles:

2.0 MeV, $\theta_P =$ $-120°$, $-145°$;

6.0 MeV, $\theta_P = -95°$, $-120°$, $-145°$;

13.0 MeV, $\theta_P = -95°$, $-120°$, $-145°$.

In addition a run was made at $\theta_F=+90°$ and $\theta_P=-70°$ for $E_B=2.0$ MeV. This corresponded to a portion of the angular range which was studied by Kamegai[3] at this energy.

The details of the equipment used and the procedures followed in acquiring and analyzing the data may be found in the Appendix.

4. RESULTS DISCUSSED

A FORTRAN IV program was written which displayed the experimental data together with the results of calculations using the theoretical model.

The format of the experimental data at each angle setting was a θ_p vs E_F contour matrix. The data for each bombarding energy were normalized using the overlapping angles of the position detector. A theoretical θ_p vs E_F matrix was constructed by calculating energy spectra for the θ_p values after correcting for the thickness of the beam-stopping foil in front of the fixed detector. The experimental and theoretical energy spectra were obtained by summing the appropriate 5° wide segments of the respective θ_p vs E_F matrices. Since the experimental measurements and the theoretical computations were concerned only with the relative values of the cross section, experiment and theory were normalized to the maximum height of the peak that corresponded to zero-momentum transfer to the target α particle (the high-energy direct peak).

The theoretical computations reproduced with reasonable accuracy the large direct interaction peaks which were found in the experimental data. The energies of the majority of the peaks were well predicted and their relative heights were fairly well predicted. In general, however, the widths of the experimental peaks were narrower than the theoretical peaks. The experimental direct peaks rose from background to their maxima and fell again below background extremely rapidly as a function of angle. Typically this range was ~40° for the high-energy direct peak and ~25° for the low-energy direct peak. This angular variation was followed very well by the theoretical model.

To be sure that the peaks attributed to direct interactions were not due to sequential decay processes, the behavior of the excited states in ^8Be which could possibly produce peaks in the region of the experimental direct peaks was carefully checked as a function of θ_p for each bombarding energy. When θ_p was plotted versus E_F, the allowed loci occurred either as straight lines (constant E_F) or as curved lines where E_F varied rapidly with small changes in θ_p. In contrast, the energies of the direct peaks changed slowly with angle in the regions where they appeared. The relative cross sections of the observed states in ^8Be were between a tenth and a twentieth of the maximum observed for the direct peaks. The states which were unambiguously identified in the experimental spectra were the 0.0-, 2.9-, 16.6-, 16.9-, and 22.5-MeV levels. Those which could occur in the region of interest were the 2.9-MeV state for $E_B = 2.0$ MeV, the 2.9-, 11.4-, and 22.5-MeV states for $E_B = 6.0$ MeV, and the 2.9-, 11.4-, 16.6-, 16.9-, and 22.5-MeV states for $E_B = 13.0$ MeV. Since the J^π of these states are 2^+ and 4^+, their relative cross sections could not have changed as rapidly with angle as did the experimental direct peaks. Moreover, peaks due to these ^8Be states should have been clearly visible for angles other than those for which the experimental direct peaks were observed. As pointed out above, most of the angular range, $0° < \theta_p < 180°$, was studied for $E_B = 6.0$ MeV and there was no indication that peaks due to these states developed an appreciable cross section for any of these angles.

As the bombarding energy changed, the levels in question came into the region of interest in different ways. There was no evidence that the ex-

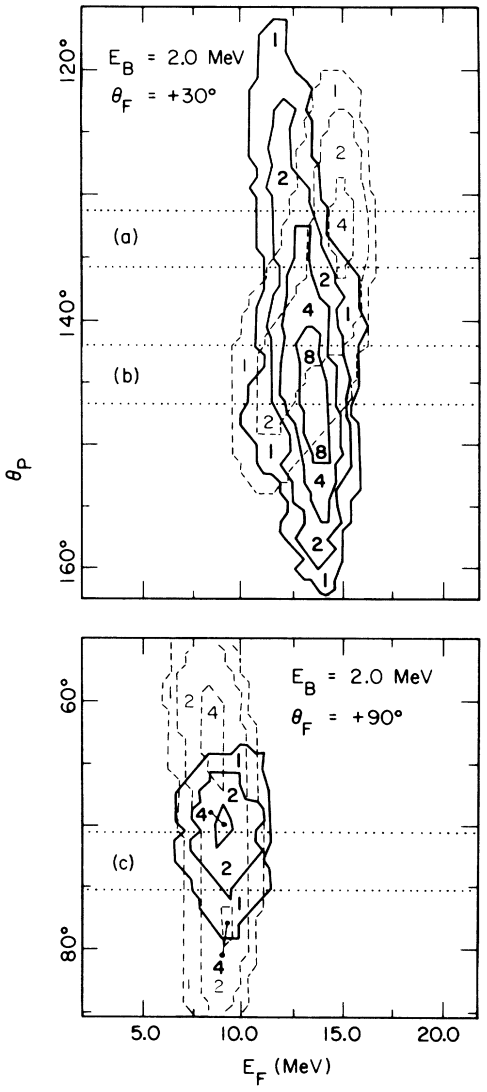

FIG. 2. Experimental (——) and theoretical (----) angle versus energy contour maps. The count level of the first contour line for $\theta_F = +30°$ is 3 counts and that for $\theta_F = +90°$ is 13 counts. Each succeeding contour line corresponds to the indicated multiple of the first count level. The areas between the dotted lines were summed to form the energy spectra shown in Fig. 3.

perimental direct peaks changed in the way that would be expected if they were due to ^{8}Be states. In addition to the detailed study made at the 2.0-, 6.0-, and 13.0-MeV bombarding energies, data were also obtained at beam energies of 4.5 and 8.0 MeV. The experimental peaks attributed to direct interactions were a prominent feature of the data for all five bombarding energies. We concluded, therefore, that the anomalous peaks which were observed were due primarily to direct interactions and not to sequential decay processes.

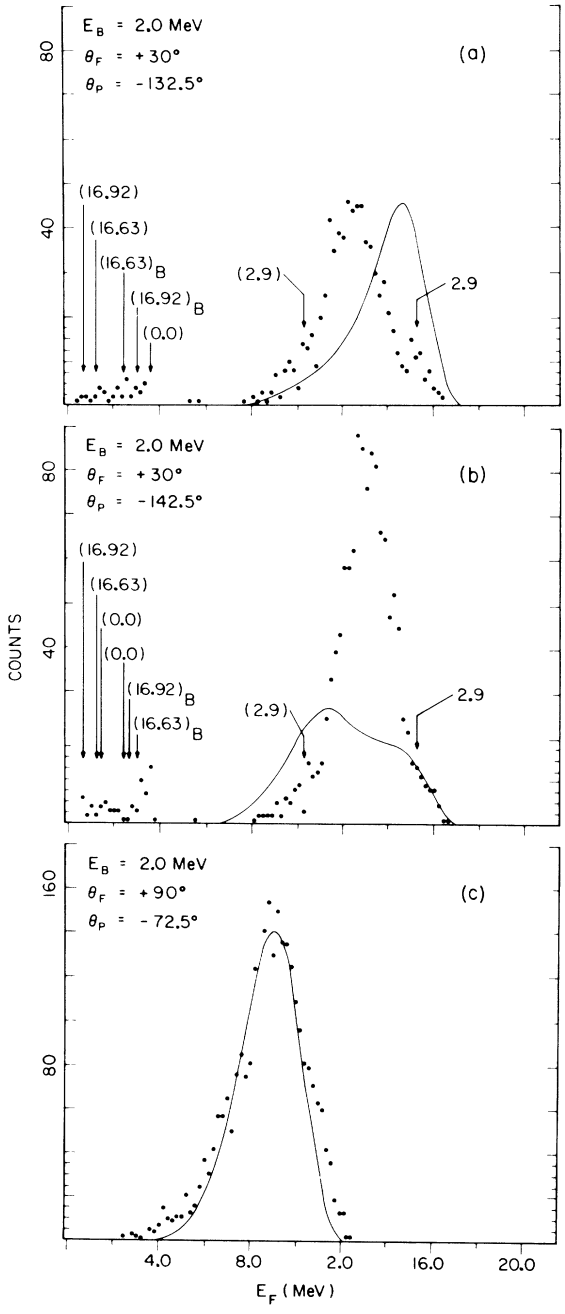

FIG. 3. (a)–(c) Experimental (....) and theoretical (——) E_F spectra. The arrows indicate the expected locations of peaks corresponding to excited states in ^{8}Be. The absence of experimental points indicates that no counts were observed.

Presentation of the Data and the Computations

The contour maps are shown in Figs. 2, 4, and 5 Solid lines were drawn through the experimental data points and dashed lines through the theoretical values. The energy scale gives the laboratory energies following the foil over the fixed detector. The angular scale gives the laboratory angles from the position detector. Figures 3 and 6 show energy spectra which were obtained by summing the 5° wide bands indicated by the dotted lines in the contour maps. Three 5° wide bands for the 6.0-MeV data are shown in Ref. 1. In these plots the experimental data points are shown together with smooth curves calculated using the theoretical model. The possible locations of peaks from the sequential decay of levels in ^{8}Be are indicated by arrows. These were calculated from three-body reaction kinematics and were corrected for the energy calibration and foil thickness of the fixed detector. The excitation values which stand alone refer to peaks formed by events in which the initial particle was incident on the fixed detector and one of the decay particles was incident on the position detector. The bracketed values correspond to peaks formed by the initial particle striking the position detector and one of the decay particles striking the fixed detector. The subscript, B, on the brackets means that both decay particles were detected, one in each detector, and the initial particle was not observed.

2.0-MeV Bombarding Energy Data

See Figs. 2 and 3. The agreement between the experimental data and the results of the theoretical model is fair for this bombarding energy. The energies of the direct interaction peaks predicted by the theoretical model differ from experiment by as much as 2.0 MeV for $\theta_F = +30°$, though for $\theta_F = +90°$, the difference is less than 0.2 MeV. However, as a function of θ_P, the experimental direct peak shows only one maximum, while the theoretical model predicts two maxima. For $\theta_F = +30°$ the energy of the experimental peak increases by about 2.0 MeV as θ_P increases. For the same range of θ_P, the energies of the theoretical peaks decrease by about 3.0 MeV as θ_P increases. A detailed comparison between the data for $\theta_F = +90°$ and the data obtained by Kamegai[3] is given in Ref. 9.

6.0-MeV Bombarding Energy Data

See Fig. 4. The good agreement between experiment and theory is evident in this case, although it should be noted that the direct interaction peaks predicted by the theoretical model are broader in both energy and angle than the direct peaks in the data. Out of the total angular range of 25 to 150° and energy from 4 to 16 MeV, the only large peaks are those shown in Fig. 4. An additional feature which is evident in the complete data is a tendency for sequential decay processes to have a smaller cross section for those angles where the direct interactions are larger. Perhaps there is some sort of interference occurring between the direct mode and the sequential processes. The smaller peaks in Fig. 4 which are not predicted by the theory and which do not seem to correspond to states in ^8Be are somewhat mysterious. Perhaps a more complete theory of the direct interaction effects could explain these peaks as well.

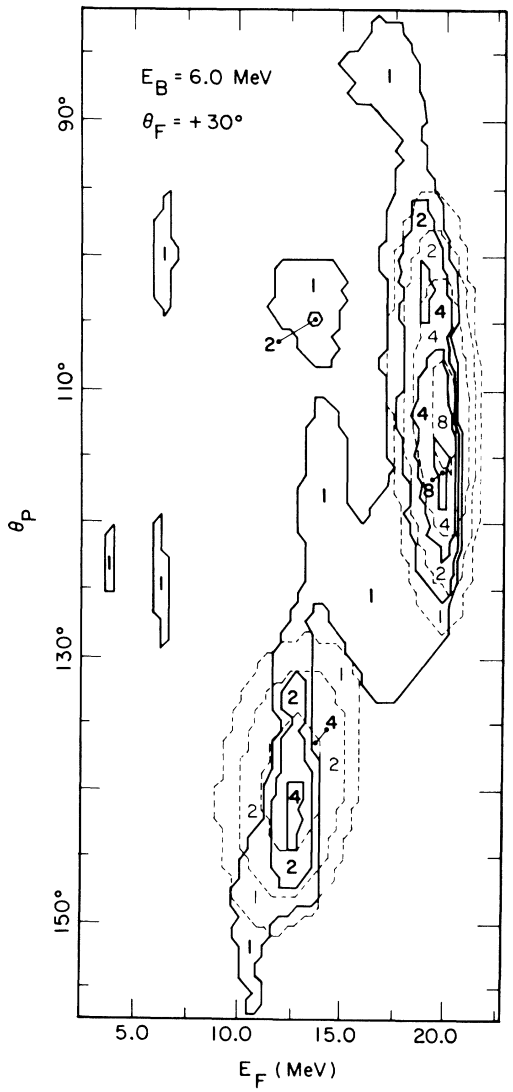

FIG. 4. Experimental (——) and theoretical (– – – –) angle versus energy contour maps. The count level of the first contour line is 91 counts. Each succeeding contour line corresponds to the indicated multiple of the first count level

13.0-MeV Bombarding Energy Data

See Figs. 5 and 6. For this bombarding energy the agreement between experiment and theory is

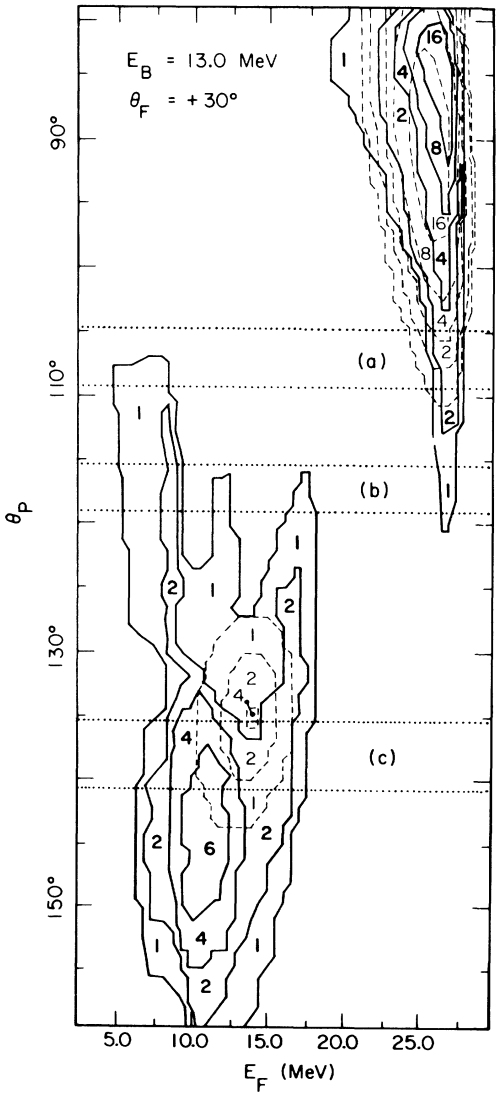

FIG. 5. Experimental (——) and theoretical (– – – –) angle versus energy contour maps. The count level of the first contour line is 17 counts. Each succeeding contour line corresponds to the indicated multiple of the first count level. The areas between the dotted lines were summed to form the energy spectra displayed in Fig. 6.

moderately good. The energy of the high-energy direct peak predicted by the theoretical model is in fairly good agreement with experiment. The energy of the experimental low-energy direct peak deviates from the prediction of the theoretical model by about 2.5 MeV and the relative peak heights disagree by a factor of 2. The magnitudes of the relative cross sections of the experimental and theoretical peaks do not change in quite the same way as θ_P changes. Again, the cross sections for the sequential decay processes decrease when the direct interaction effects become large. There are also unexplained peaks which perhaps result from more complicated direct interaction effects.

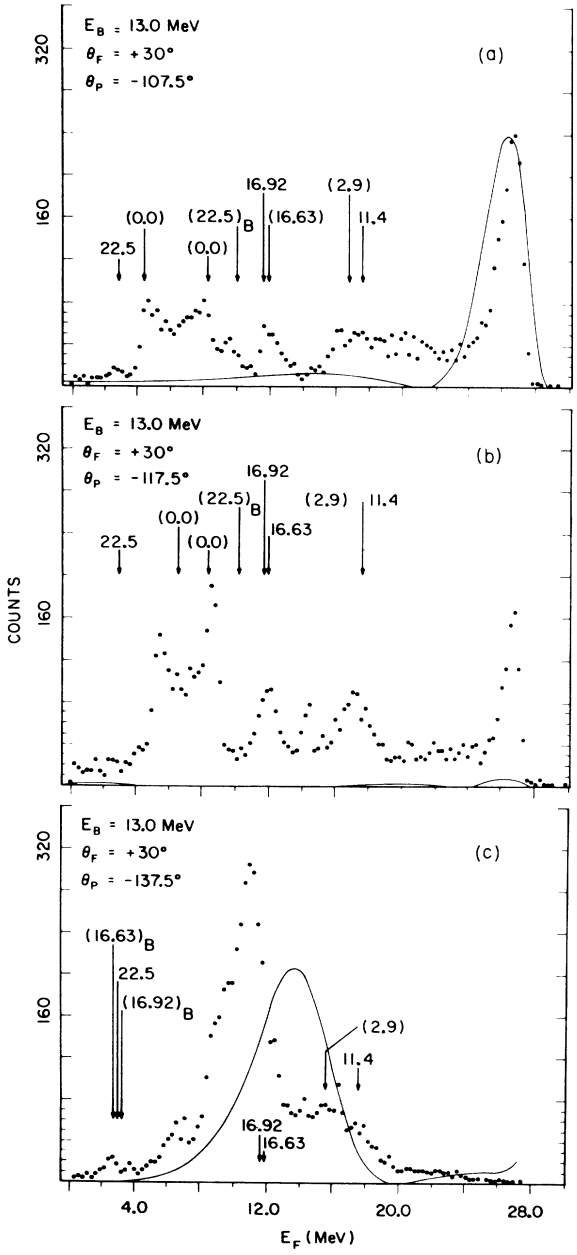

FIG. 6. (a)–(c) Experimental (····) and theoretical (——) E_F spectra. The arrows indicate expected locations of peaks corresponding to excited states in ^{8}Be.

5. CONCLUSIONS

In the 2 ^{6}Li → 3α reaction, an important contribution to the differential cross section is due to a direct interaction. The portions of the experimental energy spectra in which the direct peaks appeared were reproduced reasonably well by a theoretical model which included only the essential features of one particular type of direct reaction mechanism. Even better agreement with experiment should be possible by using more realistic nuclear potentials and by including Coulomb forces and α-α interactions.

APPENDIX. EXPERIMENTAL APPARATUS AND PROCEDURE

The ^{6}Li beam was produced by the University of Iowa's HVEC Model CN Van de Graaff positive-ion accelerator. Details concerning the beam transport system may be found in Ref. 9. The beam entering the ORTEC Model 600 scattering chamber was collimated to a maximum diameter of 3.4 mm at the target. Two target holders were used. The normal holder was used only with a radioactive source for calibration purposes. During the accelerator runs, a special holder with an integral vacuum lock was used so that metallic ^{6}Li targets could be transported from the target preparation area to the scattering chamber without exposure to the atmosphere. The targets were composed of approximately 50 μg/cm^2 of isotopically pure ^{6}Li metal which had been deposited on about 200 μg/cm^2 of copper foil.

The detector mounts were attached to rotating plates fastened to the top and bottom covers of the chamber. Two silicon surface-barrier detectors were employed in this experiment. The ORTEC 50-mm^2 fixed detector was 958 μm thick. The circular apertures of the collimator telescope to which it was fastened defined an acceptance angle of 5° at 4 cm from the center of the target. The 4×20-mm position-sensitive detector, made by Nuclear Diodes, was 240 μm thick. The rectangular aperture behind which it was mounted spanned an angular range of 7°×31° at 3 cm from the target.

Each detector was covered with aluminized Mylar foil in order to stop the scattered beam. The thickness of the Mylar was determined to be 3.36 mg/cm^2 by noting the energy loss of the 6.05-

and 8.78-MeV α particles from a thorium C (ThC) source. One thickness over each detector was sufficient for the 2.0- and 6.0-MeV runs, but a double thickness had to be used over the fixed detector for the 13.0-MeV runs.

The electronics are shown in Fig. 7. The energy signal from the position detector was derived from the front face of the detector. The position signal was taken from one end of the resistive layer on the back of the position detector. The other end of the resistive layer was grounded through a 2000-Ω metal-film resistor. This ensured that the position signals from particles incident near the grounded end of the detector were always above electronic noise and the threshold setting of the analog-to-digital converter (ADC). The energy signals, E_F and E_P, and the position signal, P_P, were initially processed by ORTEC preamplifiers and sent to Canberra linear amplifiers. E_F and E_P also went to ORTEC timing filter amplifiers which optimized the wave forms for presentation to ORTEC constant fraction timing (CFT) discriminators. For E_F the resulting pulse rise times were approximately 15 nsec. For E_P the rise times varied continuously, from about 40 nsec for particles incident near the ends of the position detector, to about 80 nsec for those striking near its center. The CFT discriminators were set for a fraction of 0.3 with shaping delays of $T_d(E_F) = 8$ nsec and $T_d(E_P) = 31$ nsec. Their timing outputs were fed to an ELRON time-to-amplitude converter (TAC) and to EG & G pileup gates.

A coincident event was assumed to have occurred when the time delay, T, between the E_F and E_P timing signals was less than 150 nsec as measured by the TAC. The T pulses were sent to a Mech-Tronics integral discriminator which put out logic pulses that opened Mech-Tronics linear gates. This allowed the E_F, E_P, P_P, and T signals to pass to Nuclear Data ADC's for analysis and subsequent storage by a Control Data computer. The pileup gates prevented the analysis of real coincident signals that had been distorted by other pulses occurring within a time interval of 11 μsec.

The amplitude and rise-time compensated timing techniques that were used in conjunction with the TAC gave excellent results. The peak-to-background ratio of the timing peak was usually greater than 150 to 1. The maximum time resolution for the whole position detector was 12.5 nsec, full width at half maximum (FWHM). The time delay had a small dependence on the location of the event in the position detector. The resolution for any 5° wide segment of the position detector was less than 5 nsec FWHM.

To establish an accurate energy calibration, the

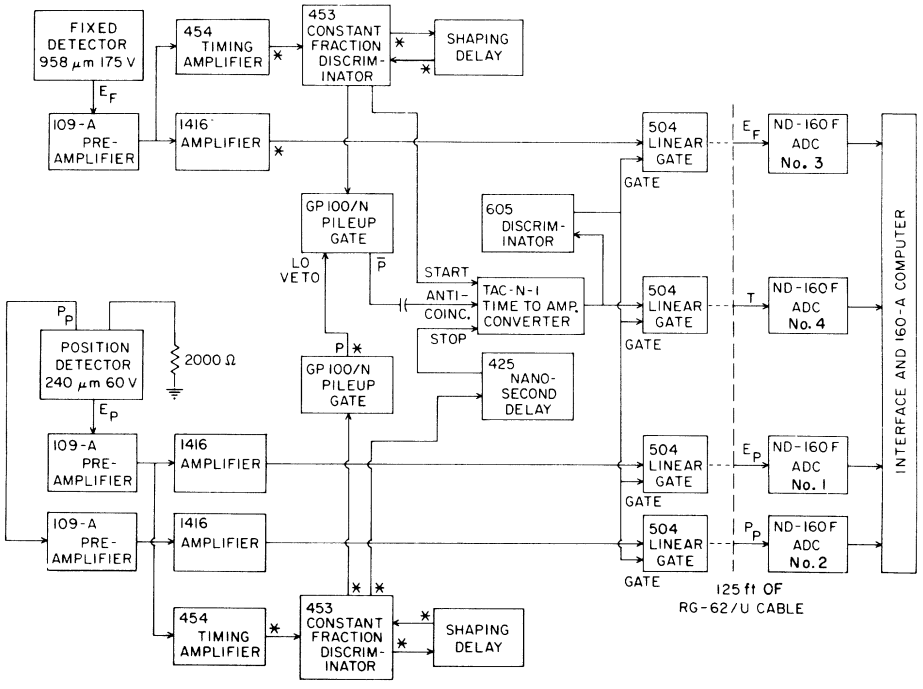

FIG. 7. Block diagram of the electronics used in this experiment. Note: All connections are RG-62/cable unless marked by a *.

detectors and the electronics were calibrated with the 6.05- and 8.78-MeV α particles from a ThC source. The zero intercept and the response linearity of the ADC's were carefully checked using a pulser. In addition, a single-parameter spectrum from the ^{6}Li + ^{6}Li reaction was recorded for the fixed detector at each energy. Several proton and deuteron groups stood well above the continuum and provided excellent calibration points.

The angular calibration of the position detector was obtained by using α particles from a ThC source and a special collimator with nine vertical slots. The slot widths and their separations were precisely measured by means of a traveling microscope.

A general purpose, four-parameter data acquisition and reduction program was used with the on-line computer to store the data on magnetic tape in time sequential fashion and to monitor the progress of the experiment. The experimental data were later completely and efficiently reduced by using the University of Iowa's IBM 360/65 computer. FORTRAN IV programs read the data, divided out the energy dependence of the position signal,[10] generated spectra of E_F, E_P, P_P, and T, and contour matrices of E_P vs E_F, P_P vs E_F, T vs E_F, P_P vs E_P, T vs E_P, and P_P vs T. The spectra and matrices were printed out and were also stored on a direct-access disk file. These reduced data and the energy and angular calibrations were used with other programs to compare the experimental data with the theoretical model.

---

*Work was supported in part by the National Science Foundation.

†Present address: Oliver Lodge Laboratory, The University of Liverpool, P.O. Box 147, Liverpool, L69 3BX, United Kingdom.

[1]A preliminary report of this work appeared in L. L. Gadeken and E. Norbeck, Phys. Rev. Letters 27, 952 (1971).

[2]R. E. Warner *et al.*, Phys. Rev. Letters 27, 961 (1971).

[3]M. Kamegai, Phys. Rev. 131, 1701 (1963).

[4]E. H. Berkowitz, Nucl. Phys. 82, 52 (1966).

[5]B. Frois *et al.*, Nucl. Phys. A153, 277 (1970).

[6]G. G. Ohlsen, Nucl. Instr. Methods 37, 240 (1965).

[7]K. Wildermuth and W. McClure, *Springer Tracts in Modern Physics* (Springer-Verlag, Berlin, 1966), Vol. 41, p. 27.

[8]F. D. Ingram and E. Norbeck, Phys. Rev. 187, 1302 (1969).

[9]L. L. Gadeken, Ph.D. thesis, University of Iowa Research Report No. 71:24, 1971 (unpublished).

[10]The position signal from the position detector was given by $P_P = (X/L)E_P$, where E_P was the energy of the event, X was the distance from the end of the detector from which the position signal was taken to the point at which the event occurred, and L was the total electrical length of the detector.